Characterising the effect of an inverter on the regulation of the AC voltage using a frequency response identification technique

Mohamed Aldarmon, Joan Marc Rodriguez, Adria Junyent-ferre
Imperial Collage London
Exhibition Rd, South Kensington, SW7 2BX
London, UK
Phone:+44(0)20 7594 6290
Mohamed.Aldarmon18@Imperial.ac.uk
https://www.imperial.ac.uk

Keywords

≪Frequency-Domain Analysis≫, ≪Converter control≫, ≪Power quality≫.

Abstract

This paper presents a methodology to obtain a small-signal characteristics of a power electronic inverter in the frequency domain. The method is based on carrying out a series of simulations to observe the response of the inverter to a small voltage disturbance. The results obtained through the method provide information about the adequacy of the controller of the inverter and how it contributes to AC voltage regulation of the network. The paper describes the methodology and illustrates its use through a study case of a low-power three-phase inverter.

Introduction

The need to meet the future net-zero carbon targets requires the integration of more renewables to the power system using power electronic devices. Voltage source inverters (VSI) are commonly used to connect new low carbon technologies (LTCs). Depending on the grid code requirements, inverters use different high-level control modes such as unity power factor or AC voltage control. Looking at the specific implementation details, different manufacturers may choose to use different Phase Locked Loop (PLL) and internal reference calculation methods. Some controller formulations are more likely to trigger instability [1] or lead to different power quality at network level (eg voltage unbalance, harmonics). Several techniques have been proposed to study these problems using black-box models of the converters in simulation or through experimental testing. This paper studies the reaction of the inverter to a small-signal disturbance injected on the voltage of the grid. The characterisation is done through a series of simulations to create a frequency response plot for different operating conditions.

The disturbance injection method is a common tool used for measuring the impedance of devices. The disturbance injection can be either in series or in parallel with the tested device and use voltage or current injection. Choosing one of the two injection types depends on the system configuration and the characteristics of the point of injection (eg a stiff voltage or current source) and the device under test [2][3]. Different types of disturbances can be used, such as sinusoidal signal [3], chirp signal [2], and a multitone signal [4]. The measured response signals (eg current, voltage) are then processed using a discrete time Fourier (DFT) to transform the time domain signal into a phasor domain. This information can then be read in the form of Bode plots or used to obtain transfer functions and impedances for different types of assessments (eg impedance-based stability [5]).

The method can be used in simulation if accurate dynamic simulation models of the device are available. This is advantageous because it can be used with black-box manufacturer models where the internal

equations of the model are not visible to the user. With adequate test equipment, the method can also be used for experimental system identification. These technique has been used to investigate and diagnose malfunctioning devices (such defected transformers and photovoltaic solar panels [6] [7] [8]). It can also be used to assess compliance of devices with power quality requirements.

In this paper we describe a method to characterise the response of an inverter based on voltage injection in series with a Thevenin equivalent of an AC network. The results shown across the paper are based on a study case for a low voltage inverter as described in the next section.

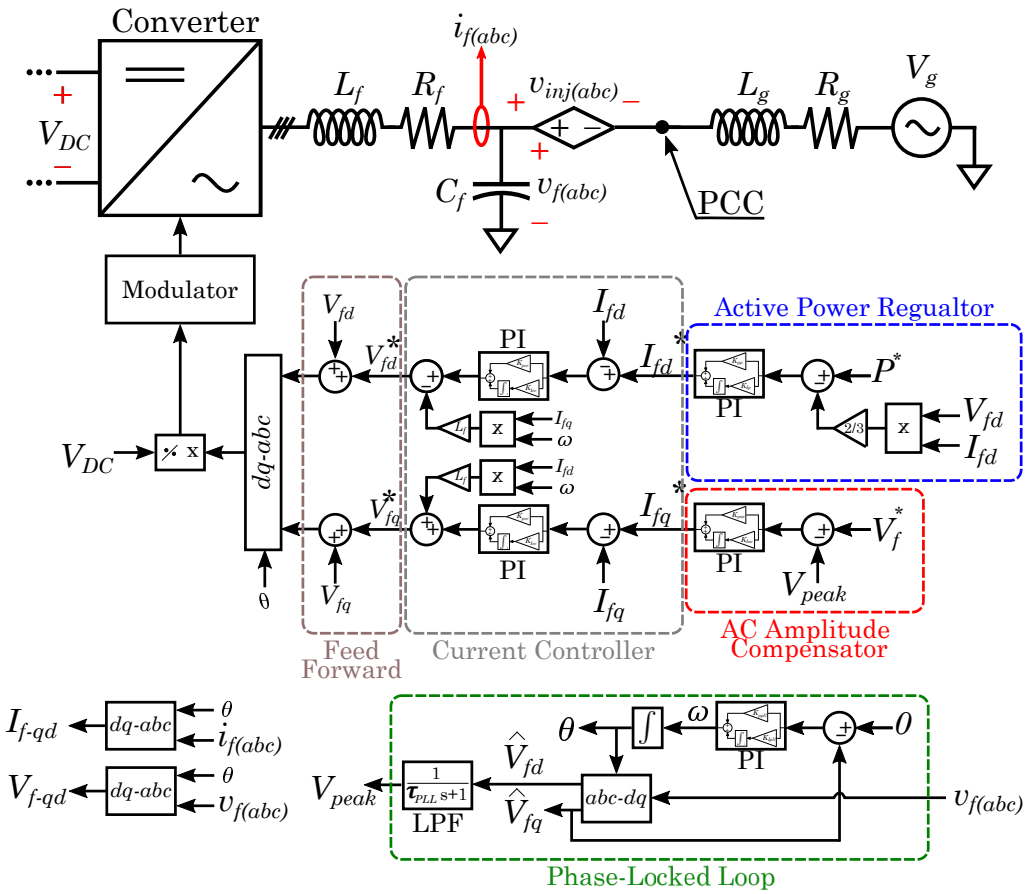

Fig. 1: Diagram of the system under test and its controller structure.

Study System

The system under the study is an inverter interfacing a DC power source (eg a solar photovoltaic DC/DC) to a distribution network. The inverter has a 2nd order LC pulse-width modulation (PWM) filter and the network is represented by a Thevenin equivalent. The injected disturbance is a small three-phase voltage in series with the Thevenin of the network. A diagram of the complete system is shown in Fig. 1. V_c is the converter voltage, v_f is the voltage of the point of common coupling (PCC), v_{inj} is the injected disturbance voltage and V_g is the grid voltage. The Thevenin equivalent of the grid has a series resistance R_g and inductance L_g. The inductance L_f of the filter has an effective series resistance (ESR) R_f, and the capacitance is C_f.

The controller of the inverter is based on a conventional synchronous reference frame vector control as shown in Fig. 1. It contains a decoupling feedback loop and a pair of Proportional Integral (PI) regulators [9]. This is nested within an active power control loop acting on the d component of the current reference and an AC voltage control loop acting on the q component both using PI controllers. A PLL fed with the voltage measured at the PCC provides information about the instantaneous modulus and angle of the positive sequence of the voltage. The angle of the positive sequence voltage is used as the angle for the Park reference frame.

The gains of the PI controllers were tuned based on the method explained in [9]. With an approximate bandwidth of 1 kHz for the current controller, 5 Hz for the PLL and 100 Hz for the power loops. All system parameters are listed in Table I.

Table I: System paramters and tuning values

Parameter	Description	Value
V_g	AC system voltage (RMS)	230 V
P	Converter rated power	50 kW
f	AC frequency	50 Hz
L_g	Grid side inductance	6.79 mH
R_g	Grid side resistance	0.2133 Ω
L_f	Inverter side inductance	8.48 mH
R_f	Inverter side resistance	53.3 mΩ
C_f	Inverter side capacitance	298 μF
τ_{cc}	Current controller time constant	0.5 ms
$K_{P_{cc}}$	Proportional gain current controller	1.6977
$K_{I_{cc}}$	Integral gain current controller	106.667
τ_{cc}	Time constant PLL loop	0.054
$K_{P_{pll}}$	Proportional gain PLL	0.1632
$K_{I_{pll}}$	Integral gain PLL	3.0219
K_{P_p}	Proportional gain power regulator	$1x10^{-3}$
K_{I_p}	Integral gain power regulator	0.042
$K_{P_{ac}}$	Proportional gain AC controller	0.5
$K_{I_{ac}}$	Integral gain AC controller	55

Furthermore, the pre-set power reference is compared with the calculated power to provide the d current reference to the inner control loop. The power is calculated from the measured current and voltage before the PCC. The voltage control loop is fed with the voltage measured at the PCC [10].

Frequency response identification methodology

In oder to obtain the system frequency response, a small-signal deviation of the steady-state operating point is caused by injecting a small voltage in series with the Thevenin equivalent of the grid. This voltage is a three-phase signal, ie for each tested frequency a voltage is injected in each of the three phases of the network with angles adjusted to have 120 degrees of difference between phases. Furthermore, the signal can be generated to contain negative or positive sequence (or both).

The frequency of the injected voltage is swept in the range between 10 Hz and 490 Hz with intermediate points generated using a logarithmic scale. For each value of frequency in the series, a frame of voltage and current data samples at 10 kHz is obtained for a duration of 0.5 s before the injection and 0.5 s in steady-state after injecting the disturbance. A Fast Fourier Transform (FFT) is applied to the data to transform the samples into phasors. The vector of *abc* voltages and currents corresponding to the specific frequency of test is multiplied by the Fortescue transformation matrix to obtain the phasors of the positive and negative sequence. The difference between the values obtained from the frame taken before and after the injection is used to eliminate the offset created on voltages and currents when operating at different power set-points.

An example of voltage at the PCC for an individual simulation is shown in Fig. 2. In this case, the voltage injected contained 1 V phase-to-phase rms of positive sequence and 1 V of negative sequence. Complete frequency response plots obtained using this method are presented for a series of scenarios of interest in the next section.

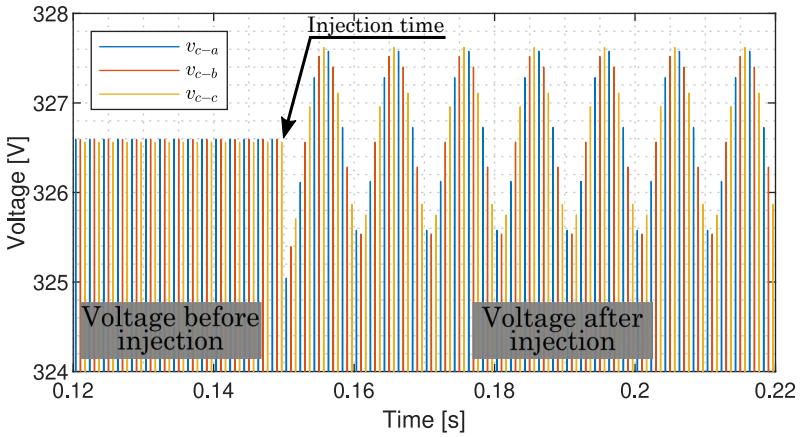

Fig. 2: Voltage at the point of common coupling upon injecting a small voltage disturbance

Case Study

The application of the proposed methodology is illustrated through a study case with three different simulation scenarios. First, the differences on the control performance observed when operating at different set-points is evaluated. The first scenario explores the effect of changing the power set-point of the converter. The second scenario investigates the operation at different AC voltage levels (see Fig.4a and 4b, respectively). The third scenario shows the impact of negative sequence voltage (see Fig. 5). The following subsections present the results obtained in detail. The values of the parameters considered in this study are summarised in Table I.

Scenario I: Varying the operating set-point

This section analyzes how the power set-point affects the system behaviour. Fig. 3b shows the performance of the *AC voltage control loop* at the base frequency of 50 Hz. This figure shows a detail of the peak of the AC voltages at the PCC before and after the disturbance. It can be seen that after the injection, the amplitude of the voltage goes through a transient excursion and finally returns to its nominal amplitude, which confirms the correct operation of the AC regulator. The diagram of the AC voltage regulator is shown in Fig. 1.

The effect of the injected voltage over the voltage measured at the PCC for different injected frequencies is shown in Fig. 3a. This plot is constructed by calculating the difference of the voltage amplitudes before and after the disturbance injection. Notice that the voltage difference at 50 Hz is zero, which means that the AC voltage regulator rejects the disturbance at nominal grid frequency as expected.

The trace in Fig. 3a also shows a resonant peak close to 350 Hz. This matches the resonant frequency of the LC filter ($f_{res} = \frac{1}{2\pi\sqrt{LC}}$), which gives 353Hz for the parameters shown in Table I.

Next, the frequency response for three different power set-points is obtained. The results are shown in Fig. 4a. This figure shows the module of the difference between the voltages before and after the injection of v_{inj}. This value would be zero if both the amplitude and the angle of the voltages before and after the injection were identical. This is not necessarily the goal of the AC voltage regulator, which only rejects the effect of the disturbance on the amplitude of the voltage. Furthermore, for all other frequencies different than zero, a value greater than one would imply that the inverter effectively amplified the effect of the disturbance on the voltage of the PCC.

It is noticed that the gain of the frequencies close to 50 Hz is not exactly 1 V. The design of the control loops (ie the PLL and the outer loops) is done such that they exhibit a low-pass behaviour. This helps neglecting disturbances above the design frequency (ie above 50 Hz). However, frequencies close to 50 Hz are not completely neglected. For instance, a 60 Hz disturbance is seen as a 10 Hz oscillation in the synchronous reference frame. Despite the low-bandwidth of the PIs in the outer loops, the low frequency ripple is still in the bandwidth of the controllers and causes the deviations observed in Fig. 4a. It is also

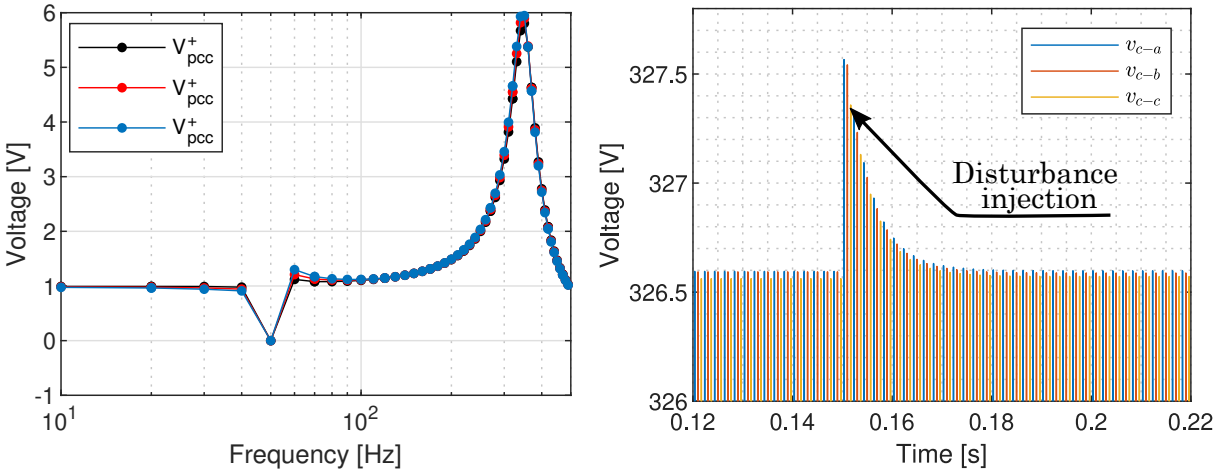

(a) Difference of voltage amplitudes at PCC.

(b) PCC voltage at injection time (f_{inj} = 50 Hz).

Fig. 3: Detail of system response at injection time (50 kW).

observed that the higher the power set-point of the converter, the larger the oscillation is seen in the $d-q$ components, which in turn impacts the voltage gain observed in the vicinity of 50 Hz.

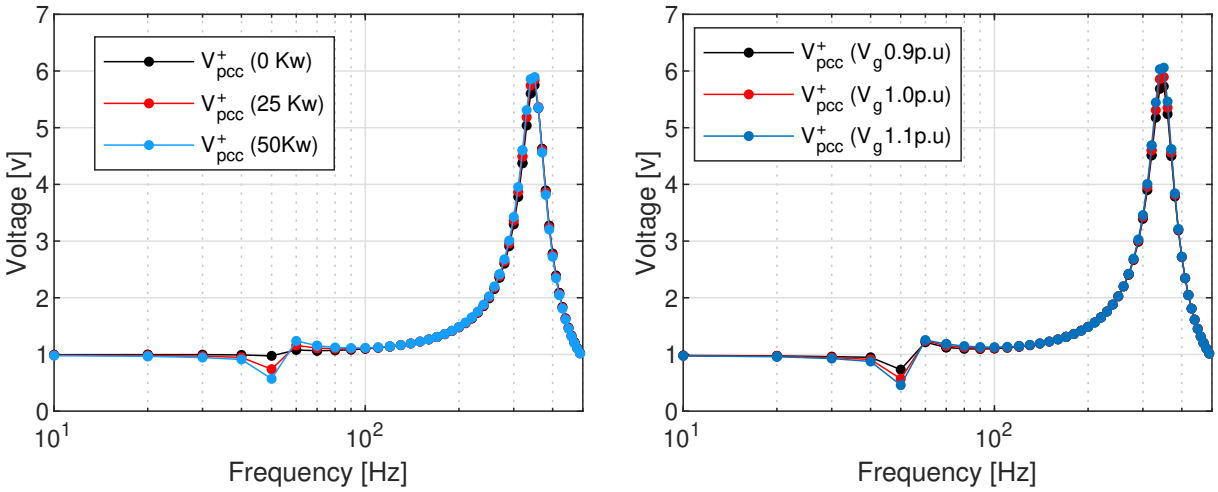

(a) Voltage response at different power set-points.

(b) Difference of voltage amplitudes at PCC (50 kW) .

Fig. 4: Frequency response information of the system.

Scenario II: Different grid voltages

In this section, the grid voltage is changed in order to investigate its effect on the inverter's response. The result is shown in Fig. 4b. Even though the variation of the AC voltage is fairly large (specifically, from -0.1 pu to +0.1 pu), the effect on the response of the system is comparatively smaller than the change observed when varying the active power set-point, with slightly larger visible effect at 50 Hz the higher the AC voltage is.

Scenario III: Impact of the negative component on the control performance

The impact of negative sequence on the response is tested next. The results are shown in Fig. 5. Here the gain on the negative sequence component of the voltage is shown together with the gain of the positive sequence. Results are obtained for different power set-points: no active power, half rated power and full rated power.

The results show that there's no visible effect of the AC voltage regulator on the negative sequence voltage. This is because the AC voltage regulator uses the amplitude of the positive sequence voltage

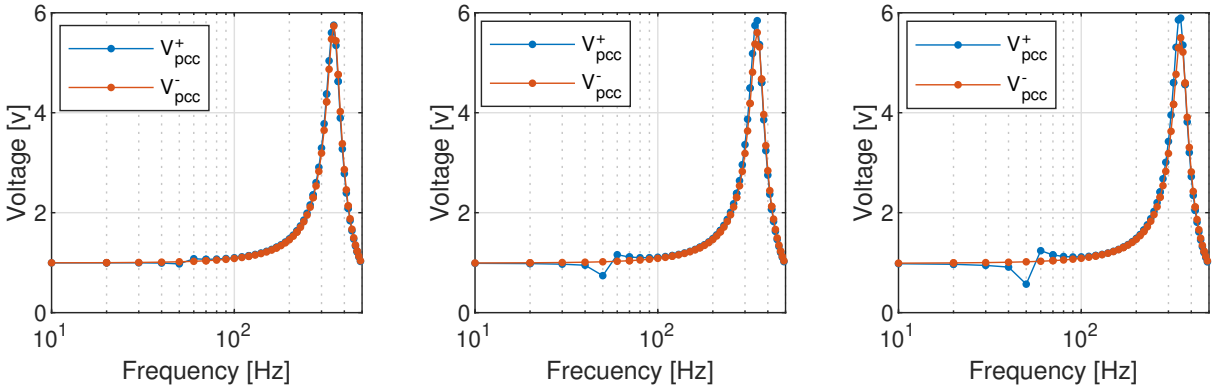

(a) Power = 0 KW (b) Power = 25 KW (c) Power = 50 KW

Fig. 5: Positive and negative voltage response

detected by the PLL, which effectively makes it ignore the negative sequence component of the voltage. Regarding the effect of changing the power set-point, here its effect on the positive sequence gain is seen as described in Scenario I, whereas no apparent change is observed on the negative sequence gain.

Conclusion

This paper has presented a method to identify how an inverter affects the voltage at its point of connection when voltages of different frequencies are injected in the equivalent model of the network. The results obtained through this method provide insights about the effectiveness of the AC voltage regulator, and the damping of the output filter of the inverter. This is useful when judging the design of the inverter hardware and its controller. The method also provides a way to judge how the converter contributes to the rejection of variations of the voltage of the network. This is desirable feature that can help improving the power quality of the voltage seen by loads connected in the vicinity of the inverter.

References

[1] M. Liserre, R. Teodorescu, and F. Blaabjerg, "Stability of photovoltaic and wind turbine grid-connected inverters for a large set of grid impedance values," *IEEE Transactions on Power Electronics*, vol. 21, no. 1, pp. 263–272, 2006.

[2] Z. Shen, M. Jaksic, P. Mattavelli, D. Boroyevich, J. Verhulst, and M. Belkhayat, "Three-phase ac system impedance measurement unit (imu) using chirp signal injection," in *2013 Twenty-Eighth Annual IEEE Applied Power Electronics Conference and Exposition (APEC)*, pp. 2666–2673, 2013.

[3] Y. Familiant, K. Corzine, J. Huang, and M. Belkhayat, "Ac impedance measurement techniques," in *IEEE International Conference on Electric Machines and Drives, 2005.*, pp. 1850–1857, 2005.

[4] M. Jaksic, Z. Shen, I. Cvetkovic, D. Boroyevich, R. Burgos, and P. Mattavelli, "Wide-bandwidth identification of small-signal dq impedances of ac power systems via single-phase series voltage injection," in *2015 17th European Conference on Power Electronics and Applications (EPE'15 ECCE-Europe)*, pp. 1–10, 2015.

[5] J. Sun, "Impedance-based stability criterion for grid-connected inverters," *IEEE Transactions on Power Electronics*, vol. 26, no. 11, pp. 3075–3078, 2011.

[6] X. Zhao, C. Yao, C. Zhang, and A. Abu-Siada, "Toward reliable interpretation of power transformer sweep frequency impedance signatures: experimental analysis," *IEEE Electrical Insulation Magazine*, vol. 34, no. 2, pp. 40–51, 2018.

[7] E. Al Murawwi and B. Barkat, "A new technique for a better sweep frequency response analysis interpretation," in *2012 IEEE International Symposium on Electrical Insulation*, pp. 366–370, 2012.

[8] K. Pourhossein and M. Asadi, "Identifying internal defects of photovoltaic panels using sweep frequency response analysis," in *2019 International Aegean Conference on Electrical Machines and Power Electronics (ACEMP) & 2019 International Conference on Optimization of Electrical and Electronic Equipment (OPTIM)*, pp. 481–485, 2019.

[9] A. Egea-Alvarez, S. Fekriasl, and O. Gomis-Bellmunt, "Advanced vector control for voltage source converters connected to weak grids," in *2016 IEEE Power and Energy Society General Meeting (PESGM)*, pp. 1–1, 2016.

[10] A. Egea-Alvarez, S. Fekriasl, F. Hassan, and O. Gomis-Bellmunt, "Advanced vector control for voltage source converters connected to weak grids," *IEEE Transactions on Power Systems*, vol. 30, no. 6, pp. 3072–3081, 2015.